Carbon 120 (2017) 11–16

Contents lists available at ScienceDirect

Carbon

journal homepage: www.elsevier.com/locate/carbon

Effect of trapped water on the frictional behavior of graphene oxide layers sliding in water environment

Jihyung Lee, Murooj Atmeh, Diana Berman*

Department of Materials Science and Engineering, University of North Texas, United States

ARTICLE INFO

Article history:
Received 26 February 2017
Received in revised form
3 May 2017
Accepted 4 May 2017
Available online 8 May 2017

ABSTRACT

Two-dimensional materials have great potential for applications in the wide-reaching areas of sensing, drug delivery, and biomolecule nano-transportation. When considering graphene for possible applications, interactions with the surrounding environment should be always kept in mind, as they can cause wear and damage of the films and thus largely affect the overall performance of graphene-based devices. In this paper, we use Quartz Crystal Microbalance (QCM) to explore interactions of graphene oxide (GO) films with water at solid/liquid interface. We demonstrate that water trapped between GO layers during deposition from the water solution largely affects the response of the QCM in the liquid environment by unexpectedly increasing the resonant frequency of oscillations. Once the trapped water is released in the DI water environment or eliminated in case of graphene deposited from an ethanol solution, the resonant frequency decreases upon immersion as predicted from viscosity effect on the oscillations. The trapped water also increases friction against the QCM movement in the liquid environment, as indicated by 2–3 times larger mechanical resistance values. Our observations confirm the importance of GO composition and deposition procedures and propose a new method for releasing the trapped water from the structures and improving the tribological performance of the film in solid/liquid interface.

1. Introduction

The discovery of graphene, the two-dimensional form of carbon, attracted lots of attention to the new class of atomically thin films, which demonstrate specific structures and unique properties [1]. Transmission Electron Microscopy (TEM) confirmed that graphene can be used as a protective membrane to study the interactions of biological cells [2,3]. Graphene has seen applications as an electrochemical platform to sense explosive compounds [4] or biological species [5] and as an electrode material in batteries [6]. An important aspect of these potential applications is graphene immersed in a liquid. In this case, the surrounding liquid tends to largely impact the performance and reliability of graphene-based devices.

2D materials demonstrate their own unique way for interacting with water. Algara-Siller et al. showed that residual water molecules, locked between two graphene sheets, arrange into a new form of two-dimensional ice, 'square ice', at room temperature [7]. Ma et al. revealed that propagating thermal ripples in graphene lead to fast diffusion of water along the graphene plane [8]. It was also demonstrated that in contrast to classical interactions of water with solids, the retention force of water on chemically homogeneous graphene does not vary with the drop resting time [9]. Moreover, though the contact angle between the water and graphene is dependent on the substrate material [10], introducing graphene film on the rough surface prevents water penetration into surface defects and thus increases its mobility on the surface [11]. Despite the numerous efforts in understanding all the fundamental aspects of the material property and behavior, some basic questions on the tribology of water sliding on graphene and graphene oxide surface remain unexplored.

In the majority of the existing tribological studies, when graphene is deposited at the sliding interface, only the solid/solid contact is examined [12–15]. Meanwhile, quantitative estimation for liquid layers sliding on the graphene surface is limited to the available measurement techniques.

Previous studies demonstrated the unique sensitivity of Quartz Crystal Microbalance (QCM) to non-destructively reproduce in resonant frequency and amplitude feedback the smallest changes in contact mechanics and the surface morphology of QCM

* Corresponding author.
E-mail address: Diana.Berman@unt.edu (D. Berman).

http://dx.doi.org/10.1016/j.carbon.2017.05.008
0008-6223/

electrodes [16,17]. The physics of these interactions shows that when the adsorbed layers are not attached rigidly to the surface of electrodes, interfacial slip may occur as a result of extreme shear vibrations. Modulations in frequency and amplitude due to layers sliding on the QCM uncover new possibilities to evaluate tribological behavior at the sliding interface [18]. Even smallest changes in the morphology of QCM can be thus detected [19,20]. Previous studies have used QCM to study interactions of graphene with adsorbed monolayers of krypton [21].

In this paper, we suggest using QCM technique for evaluating the mechanical resistance of water sliding on graphene oxide film, and thus for understanding the friction of sliding liquid layers on graphene at the solid/liquid interface. Previous results have indicated the tendency of graphene to convert into graphene oxide in a water environment [22]; therefore, to avoid graphene chemistry changes during oscillation, initial samples were already oxidized.

2. Experimental procedure

In the QCM, a single crystal of quartz oscillates at an extremely sharp resonance frequency, on the order of several MHz, with very little internal energy dissipation. These oscillations are driven by applying the electrical potential difference to the metal electrodes deposited on the surface of the quartz.

When the adsorbed film is rigidly attached to the QCM electrodes, the change in frequency (δf_{film}) of QCM is negative and can be calculated by the following Eq. (1) [23]:

$$\delta f_{film} = -\frac{2f^2}{A\sqrt{\rho_q \mu_q}}\Delta m \tag{1}$$

where f is the fundamental frequency of the QCM, Δm is mass change, A is the surface area of QCM, $\rho_q = 2648\ \mathrm{kg/m^3}$ is the density of quartz, and $\mu_q = 2.947 \times 10^6\ \mathrm{kg} \times \mathrm{m/s^2}$ is the shear modulus of quartz.

When the QCM is oscillating in the viscous liquid environment, its frequency is also affected by the properties of the surrounding matter and slippage of the adsorbed layers on the QCM surface [24]:

$$\delta f_{film} = -f^{3/2}\sqrt{\frac{\rho_L \eta_L}{\pi \mu_q \rho_q}} \tag{2}$$

where ρ_L and η_L are the density and viscosity of the liquid, correspondingly.

By substituting the values into Eq. (2), the calculated change in resonant frequency when the QCM is immersed in water should be negative and approximately $\delta f = -(715 \pm 10)$ Hz.

The mechanical resistance measured in Ohms is the resistance to be added to the oscillator circuit to sustain stable QCM oscillations [25]. For the QCM immersed in liquid, the mechanical resistance is [26]:

$$\Delta R = (2fL_u)\sqrt{\frac{4\pi f \rho_L \eta_L}{\mu_q \rho_q}} \tag{3}$$

where L_u is inductance for the dry resonator. Mechanical resistance for a clean gold electrode QCM immersed in water should be around 400 Ω.

To investigate the effect of water on the level of interactions of graphene with liquid environment, 2.5-cm diameter QCMs with 1.3-cm diameter gold-plated electrodes were used. The resonant frequency for the monitors chosen was around 5 MHz. Graphene oxide layers were deposited from water containing (water GO) and ethanol (ethanol GO) containing solutions of 5 g/L concentration (purchased from Graphene Supermarket). One drop of the solution was drop-casted onto the gold surface of the QCM electrode, and the liquid was evaporated for 3 h in a dry nitrogen atmosphere. Heating of the samples was performed on a hot plate at 110 °C for 10 min. Based on the coverage area and considering the bulk density of the materials to be ~1 g/cm3, the estimated thickness of resulting graphene oxide film is ~300 nm. Therefore, the resulting graphene oxide films were rather thick and, based on the previous funding of the substrate effect on graphene/water interactions [10], the effect of the substrate on the friction measurements can be neglected.

Changes in QCM resonant frequency and mechanical resistance of oscillations were monitored using the SRS QCM 200 system. The specifically designed holder allows contact of the QCM with the liquid only at one side, while the second electrode and electric connections are kept isolated from water. When the samples were immersed in a liquid environment, resonant frequency and resistance were monitored after an initial 60 s equilibration period.

Scanning Electron Microscope (SEM) images of GO deposited from water and ethanol solution were collected with an FEI NOVA 200 system. Raman spectra of the resulting films were collected using Nicolet Almega XR Dispersive Raman spectrometer with green-light laser ($\lambda = 532$ nm). Additionally, the atomic concentration of oxygen in graphene oxide samples has been evaluated using PHI 5000 Versaprobe Scanning X-ray Photoelectron Spectroscopy (XPS). Changes in the water amount were estimated using a Nicolet 6700 Fourier Transformation Infrared spectrometer (FTIR) with 600–4000 $\mathrm{cm^{-1}}$ spectral range. The hydrophilicity/hydrophobicity of the surface after graphene oxide deposition was measured using the sessile water drop method of contact angle goniometers (Ramé-hart 250).

3. Results and discussion

To investigate the interactions of graphene with water, we prepared samples of graphene oxide from a water solution and from an ethanol solution. Fig. 1(a) and (b) highlight the original coverage of the graphene samples on the gold electrode surface. Raman analysis of the samples indicates the characteristic for graphene oxide D (at ~1300 $\mathrm{cm^{-1}}$), G (at ~1560 $\mathrm{cm^{-1}}$), and 2D (at ~2700 $\mathrm{cm^{-1}}$) peaks [27,28]. In case of deposition from the ethanol solution, 2D peak is much higher. We attribute such differences to the fact that graphene oxide from water solution used in our experiments has higher degree of oxidation than the one from the ethanol solution. Moreover, SEM images indicate more flat nature of the as-deposited graphene oxide from ethanol, while the graphene oxide from water looks wavy and not conformally coating the surface. We further confirm oxygen content for both of the samples using XPS analysis (Fig. 1(c) and (d)). Results demonstrate higher content of oxygen in case of water solution.

Interestingly, the different methods of graphene oxide deposition resulted in completely different tendencies for resonant frequency changes (Fig. 1(e)). Graphene oxide deposited from an ethanol solution and immersed in water resulted in a negative frequency shift, as expected from Eq. (2); while graphene oxide deposited from a water solution exhibited an increase in the resulting resonant frequency of the sample immersed in water.

Fig. 2 demonstrates the typical behavior of resonant frequency (change in frequency relative to the value at time = 0) and mechanical resistance to sliding for two types of graphene oxide deposited. During initial sliding, graphene oxide from ethanol tends to adsorb small amounts of water (initial decrease in frequency and increase mechanical resistance to sliding) with partial delamination of graphene from the QCM surface afterwards

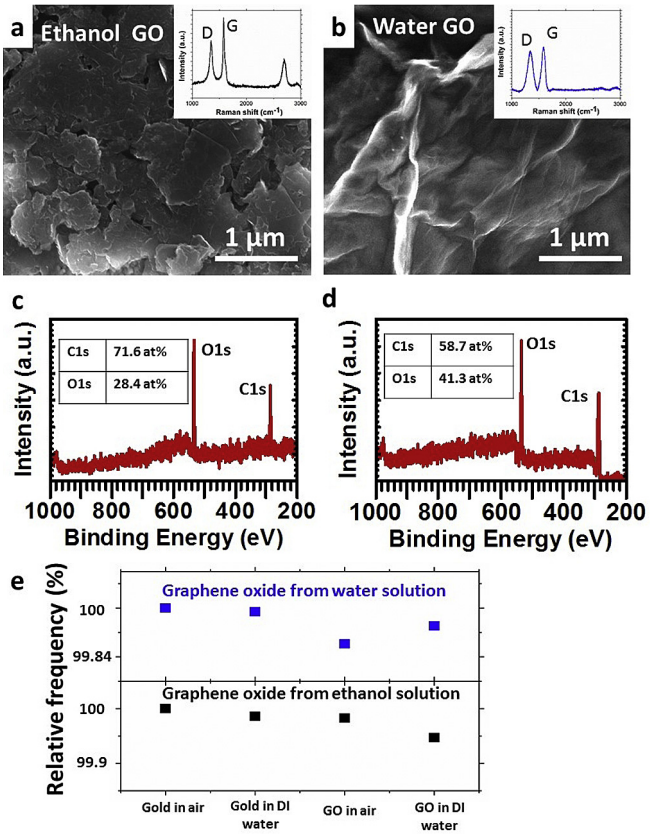

Fig. 1. The difference in the deposition method for graphene oxide is captured through the QCM resonant frequency. SEM and Raman images are presented for (a) graphene oxide from ethanol solution and (b) graphene oxide from water solution. XPS analysis of two graphene oxide samples from ethanol (c) and water (d) with the relative amount of oxygen is provided. (e) Changes in the resonant frequency of graphene coated QCM samples are presented relative to the initial resonant frequency of QCM with gold electrodes oscillating in air. The results for graphene oxide immersed in water are opposite for water-deposited and ethanol-deposited samples. (A colour version of this figure can be viewed online.)

(subsequent increase in frequency of oscillations). Interestingly, the comparatively stable behavior of graphene deposited from a water solution after immersion in water thus indicates no capability for further water adsorption, once the system was equilibrated for initial 60s of sliding.

To explore this phenomenon further and to understand the effect of the trapped water, we performed a sequence of experiments with water-deposited graphene oxide (Fig. 3). Resonant frequency and mechanical resistance of the oscillations were monitored for the graphene oxide sample initially in air (step 3), immersed for the first time in DI water (step 4), in air after DI water (step 5), second run in DI water (step 6), heated at 110 °C for 10 min (step 7), and immersed in DI water again (step 8). Note that the abnormal behavior of graphene oxide in water was observed only during initial immersion and drying afterwards. Subsequent immersion of graphene oxide follows the expected from Eq. (2) negative resonant frequency change. Such an observation proofs the assumption that initial immersion of graphene oxide in water helps to release the trapped water and ensures better adhesion of graphene oxide to the gold electrode. Subsequent heating of the sample at 110 °C increases resonant frequency slightly by evaporating any residual adsorbed water on the surface.

This observation is attributed to trapped water between graphene oxide layers which is a consequence of the deposition procedure through the solution drop-casting. Specifically, faster drying on the edges of the flakes results in higher adhesion of graphene oxide to the substrate and prevents escaping of the residual water from the middle of the flake. When this graphene is immersed in liquid, trapped water initiates decoupling of the graphene film from the QCM surface. Therefore, slippage of water-rich graphene is expected to increase resonant frequency and mechanical resistance of QCM oscillations. The end result is oscillation of QCM in a graphene + water viscous environment proximate to the surface. The higher degree of interactions of the graphene oxide layer with the liquid medium is responsible for the observed changes in resonant frequency and mechanical resistance of oscillations [29]. Once the sample is immersed for the first time, partial delamination relaxes the flakes and allows easier escape of the confined water. After drying the sample graphene oxide relaxes on the QCM surface and the subsequent immersion in water follows the regular negative frequency change.

Monitoring the mechanical resistance for sample oscillations in air and water (Fig. 3(b)) further supports our conclusion. Detachment of graphene oxide during initial immersion in the liquid environment increases resistance to oscillations at the solid/liquid

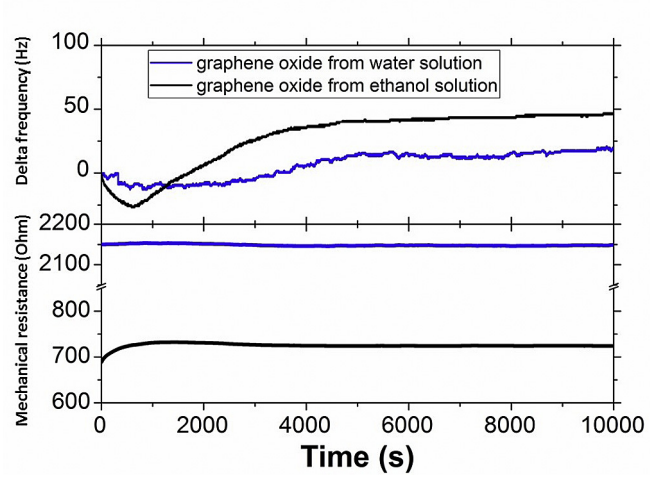

Fig. 2. Typical changes in frequency and mechanical resistance to oscillations in water environment for QCM deposited from water and ethanol solutions. Mechanical resistance for water-deposited graphene oxide upon immersion in water is 3 times larger in comparison to ethanol-deposited. The difference is attributed to trapped-water initiated decoupling of graphene oxide from the QCM surface and slipping on the surface. (A colour version of this figure can be viewed online.)

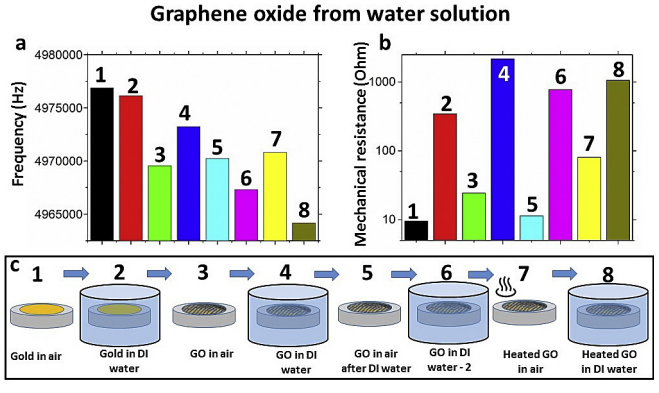

Fig. 3. Detailed monitoring of QCM with water-deposited graphene oxide (a) resonant frequency and (b) mechanical resistance of oscillations. (c) Schematic of the experimental steps is provided. Water-deposited graphene oxide shows the expected from Eq. (2) negative change in resonant frequency behavior once the water trapped between graphene oxide layers is released during initial immersion in water. (A colour version of this figure can be viewed online.)

interface of QCM/water. Subsequent immersion of graphene oxide for the second and third times decreases the viscous resistance of water during oscillation, though the level of graphene interactions with water is still larger than for the gold sample.

Based on air frequency changes, using Eq. (1), Table 1 summarizes the calculated amount of graphene oxide and water on the gold QCM surface. The adsorbed graphene oxide mass is calculated based on the assumption that all water is evaporated during baking. The results indicate that approximately half of the trapped water is released during immersion. An important point is that, some graphene oxide can be lost during first immersion into water. However, both resonant frequency and mechanical resistance demonstrate very stable behavior (Fig. 2) indicating that process of graphene release either happens immediately or can be neglected. We expect that release of graphene would happen if graphene oxide is immersed in water for long period of time, comparable with time required for water-based exfoliation process [30].

Measuring the exact amount of trapped water is challenging due to the fact that water also sits on the surface of the QCM when drying the sample after initial immersion. The major conclusion here, therefore, is that relaxed graphene oxide layer after initial immersion demonstrates much lower level of interactions with liquid environment, as depicted from reduction in the resonant frequency and mechanical resistance of oscillations. Additional Sample 2 for water-GO before and after baking has been prepared to demonstrate that amount of trapped water is rather large.

Interestingly, leaving the graphene + trapped water sample in the nitrogen atmosphere for eight days resulted in resonant frequency decrease of only 50 Hz, which indicates almost negligible water evaporation. We attribute such a slow evaporation to theoretically predicted slow diffusion of water between graphene oxide layers [31]. Only full immersion of the sample allowed quick release of the substantial amount of water.

Changes in the mechanical resistance of oscillations (Fig. 3(b)) confirm that the values are much larger than the predicted mechanical resistance of water of ~400 Ohm. Equation (3) neglects the effect of the solid/liquid interface interactions; in particular, the effect of hydrophilicity and hydrophobicity of the surface. We expect that the modifications of surface chemistry caused by the introduction of the graphene oxide should affect overall sliding of the liquid on the graphene surface. Fig. 4 summarizes contact angle measurements for bare gold and for graphene after initial drying for 3 h and after immersion in water and subsequent heating. Contact angle measurements indicate higher hydrophilicity of the graphene oxide samples compared to gold. Moreover, within the graphene oxide samples, the lowest water drop contact angle of the RT evaporated graphene oxide shows the largest degree of interactions and rapid relaxation of water layers on the surface of graphene oxide with trapped water. The large thickness of graphene oxide films also eliminates the influence of the substrate, which was shown before to greatly affect the wetting angle of water [10].

In contrast, graphene oxide deposited from the ethanol solution demonstrates regular frequency (negative change) and mechanical resistance response to oscillations in water environment. Fig. 5 summarizes the results for ethanol-based graphene oxide and indicates the values for the contact angle similar to heated or water released graphene oxide from the water solution. Mechanical resistance to oscillations demonstrates similar values as for water-deposited graphene oxide after trapped water release.

We also collected FTIR spectra of both graphene oxide samples to confirm water trapped between the layers in the case of water-deposited graphene oxide (Fig. 6). FTIR spectra analysis for graphene oxide deposited from water solution before and after immersion into DI water indicates reduction in C–OH groups (~1150 cm^{-1}) [32] and H_2O (in the region of 3400–3600 cm^{-1}) [33].

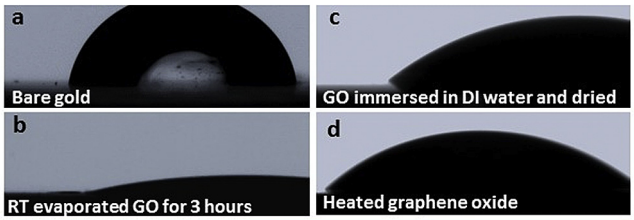

Sample	Contact angle
Bare gold	80.2° ± 0.2°
RT evaporated GO	14.7° ± 0.5°
GO immersed in DI water and dried	36.4° ± 0.7°
Heated graphene oxide	39.2° ± 0.6°

Fig. 4. Water drop contact angle measurements for (a) bare gold, (b) room temperature evaporated water-deposited graphene oxide, (c) graphene oxide dried after immersing in water, and (d) heated graphene oxide. The table summarizes the results for contact angle measurements. (A colour version of this figure can be viewed online.)

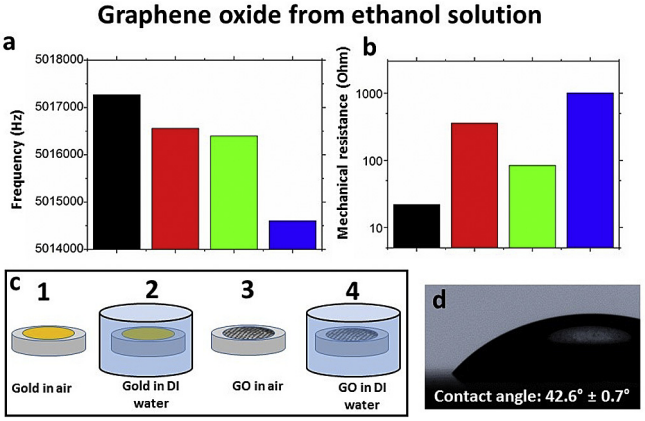

Fig. 5. Summary of test performed using ethanol-deposited graphene oxide. (a) Resonant frequency monitoring indicates the regular trend of decreasing resonant frequency with added graphene oxide, and even further decrease water immersion. (b) Resistance to the QCM oscillations is demonstrated. (c) Schematic of the experiments summarizes the steps performed. (d) Measurements of the graphene oxide contact angle indicate values similar to graphene oxide from water after baking. (A colour version of this figure can be viewed online.)

Table 1
Graphene oxide and trapped water weight for Sample 1 monitored during immersion to water and Sample 2 monitored without immersion in water.

Material deposited	Observed delta frequency	Adsorbed mass of graphene oxide	Adsorbed mass of water
Sample 1: Water-GO initial	−7374.08	3.39×10^{-4}g	0.67×10^{-4}g
Sample 1: Water-GO after water release	−6632.71	3.39×10^{-4}g	0.32×10^{-4}g
Sample 1: Water-GO after baking	−6057.73	3.39×10^{-4}g	0 g
Sample 2: Water-GO initial	−7808.49	2.97×10^{-4}g	1.32×10^{-4}g
Sample 2: Water-GO after baking	−5408.51	2.97×10^{-4}g	0 g

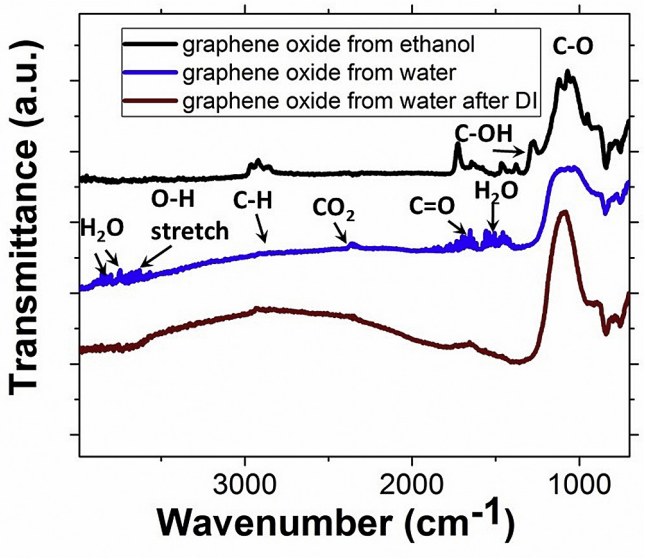

Fig. 6. FTIR spectra for graphene oxide deposited from water and ethanol solutions. The major peaks indicate the presence of residual water in water-deposited graphene oxide film. Specifically, a number of the water peaks at ~3600-3700 cm^{-1} region are observed only for the water-deposited graphene oxide. (A colour version of this figure can be viewed online.)

Extra precautions were taken when collecting FTIR spectra for the same sample of water-GO before and after immersion in water to confirm the exact position for the measurements. Though the majority of trapped water is released, existence of low-intensity peaks is attributed to the water remain on the surface of graphene oxide due to full sample immersion. In comparison, graphene deposited from ethanol solution has a higher presence of C—H bonds, though water is not present.

4. Conclusions

A series of experiments were performed to test the interactions of graphene oxide with water at solid/liquid interface using Quartz Crystal Microbalance technique. Our findings indicate that water encapsulation between graphene oxide layers during deposition procedure significantly affects both the resonant frequency and mechanical resistance of QCM oscillations. Specifically, water encapsulation causes partial delamination of GO layers and results in decoupling of the film from the oscillations. Mechanical resistance of the oscillations in this case increases 2–3 times in comparison to water-free graphene. Immersing the graphene oxide sample in a liquid environment helps to partially release the trapped water and to ensure better adhesion of graphene oxide to gold electrode of QCM. The observed during the first water immersion increases in frequency and mechanical resistance are thus attributed to partial decoupling of graphene oxide films with intercalated water acting as a lubricant for slippage in-between layers to occur. Release of the trapped water also reduces mechanical resistance to the oscillations and decreases the hydrophilicity of the graphene surface. In case of graphene oxide deposited from ethanol solution, hydrophilicity of the samples is smaller from the beginning as is the mechanical resistance of QCM oscillations in a liquid environment. Our conclusions confirm the importance of GO composition and deposition procedures and give us the confidence to propose a new method for releasing trapped water from the structures and thereby improving the tribological performance of the film in a solid/liquid interface.

Acknowledgements

The authors thank Dr. Rick Reidy for fruitful discussions and for his help with water droplet contact angle measurements. Support from Advanced Materials and Manufacturing Processes Institute (AMMPI) is acknowledged. This work was performed in part at the University of North Texas's Materials Research Facility.

References

[1] A.K. Geim, K.S. Novoselov, The rise of graphene, Nat. Mater 6 (2007) 183–191.
[2] C. Wang, Q. Qiao, T. Shokuhfar, R.F. Klie, High-resolution electron microscopy and spectroscopy of ferritin in biocompatible graphene liquid cells and graphene sandwiches, Adv. Mater. 26 (2014) 3410–3414.
[3] Q. Chen, J.M. Smith, J. Park, K. Kim, D. Ho, H.I. Rasool, A. Zettl, A.P. Alivisatos, 3D motion of DNA-Au nanoconjugates in graphene liquid cell electron microscopy, Nano Lett. 13 (2013) 4556–4561.
[4] L. Tang, H. Feng, J. Cheng, J. Li, Uniform and rich-wrinkled electrophoretic deposited graphene film: a robust electrochemical platform for TNT sensing, Chem. Commun. 46 (2010) 5882–5884.
[5] Y. Wang, Y. Li, L. Tang, J. Lu, J. Li, Application of graphene-modified electrode for selective detection of dopamine, Electrochem. Commun. 11 (2009) 889–892.
[6] J. Xiao, D. Mei, X. Li, W. Xu, D. Wang, G.L. Graff, W.D. Bennett, Z. Nie, L.V. Saraf, I.A. Aksay, J. Liu, J.-G. Zhang, Hierarchically porous graphene as a lithium–air battery electrode, Nano Lett. 11 (2011) 5071–5078.
[7] G. Algara-Siller, O. Lehtinen, F.C. Wang, R.R. Nair, U. Kaiser, H.A. Wu, A.K. Geim, I.V. Grigorieva, Square ice in graphene nanocapillaries, Nature 519 (2015) 443–445.
[8] M. Ma, G. Tocci, A. Michaelides, G. Aeppli, Fast diffusion of water nanodroplets on graphene, Nat. Mater 15 (2016) 66–71.
[9] H.E. N'guessan, A. Leh, P. Cox, P. Bahadur, R. Tadmor, P. Patra, R. Vajtai, P.M. Ajayan, P. Wasnik, Water tribology on graphene, Nat. Commun. 3 (2012) 1242.
[10] J. Rafiee, X. Mi, H. Gullapalli, A.V. Thomas, F. Yavari, Y. Shi, P.M. Ajayan, N.A. Koratkar, Wetting transparency of graphene, Nat. Mater 11 (2012) 217–222.
[11] E. Singh, A.V. Thomas, R. Mukherjee, X. Mi, F. Houshmand, Y. Peles, Y. Shi, N. Koratkar, Graphene Drape Minimizes the Pinning and hysteresis of water drops on nanotextured rough surfaces, ACS Nano 7 (2013) 3512–3521.
[12] D. Berman, S.A. Deshmukh, S.K.R.S. Sankaranarayanan, A. Erdemir, A.V. Sumant, Extraordinary macroscale wear resistance of one atom thick graphene layer, Adv. Funct. Mater. 24 (2014) 6640–6646.
[13] D. Berman, S.A. Deshmukh, S.K.R.S. Sankaranarayanan, A. Erdemir, A.V. Sumant, Macroscale superlubricity enabled by graphene nanoscroll formation, Science 348 (2015) 1118–1122.
[14] D. Berman, A. Erdemir, A.V. Sumant, Graphene: a new emerging lubricant, Mater. Today 17 (2014) 31–42.
[15] D. Berman, A. Erdemir, A.V. Sumant, Few layer graphene to reduce wear and friction on sliding steel surfaces, Carbon 54 (2013) 454–459.
[16] A. Kubono, Y. Minagawa, T. Ito, In situ study on layer-by-layer growth in vapor deposition of linear long-chain molecules using a quartz crystal microbalance, J. Appl. Phys. 114 (2013).
[17] S.J. Martin, R.W. Cernosek, J.J. Spates, Sensing liquid properties with shear-mode resonator sensors, solid-state sensors and actuators, 1995 and Eurosensors IX, in: Transducers '95, the 8th International Conference on, 1995, pp. 712–715.
[18] J. Krim, A. Widom, Damping of a crystal oscillator by an adsorbed monolayer and its relation to interfacial viscosity, Phys. Rev. B 38 (1988) 12184–12189.
[19] D. Berman, J. Krim, Impact of oxygen and argon plasma exposure on the roughness of gold film surfaces, Thin Solid Films 520 (2012) 6201–6206.
[20] M. Pierno, L. Bignardi, M.C. Righi, L. Bruschi, S. Gottardi, M. Stohr, O. Ivashenko, P.L. Silvestrelli, P. Rudolf, G. Mistura, Thermolubricity of gas monolayers on graphene, Nanoscale 6 (2014) 8062–8067.
[21] M. Walker, C. Jaye, J. Krim, M.W. Cole, Frictional temperature rise in a sliding physisorbed monolayer of Kr/graphene, J. Phys-Condens Mat. 24 (2012).
[22] J. Chen, Y. Zhang, M. Zhang, B. Yao, Y. Li, L. Huang, C. Li, G. Shi, Water-enhanced oxidation of graphite to graphene oxide with controlled species of oxygenated groups, Chem. Sci. 7 (2016) 1874–1881.
[23] G. Sauerbrey, Verwendung von Schwingquarzen zur Wägung dünner Schichten und zur Mikrowägung, Z. für Phys. 155 (1959) 206–222.
[24] K.K. Kanazawa, J.G. Gordon, Frequency of a quartz microbalance in contact with liquid, Anal. Chem. 57 (1985) 1770–1771.
[25] A. Arnau, T. Sogorb, Y. Jiménez, Circuit for continuous motional series resonant frequency and motional resistance monitoring of quartz crystal resonators by parallel capacitance compensation, Rev. Sci. Instrum. 73 (2002) 2724–2737.
[26] S.J. Martin, V.E. Granstaff, G.C. Frye, Characterization of a quartz crystal microbalance with simultaneous mass and liquid loading, Anal. Chem. 63 (1991) 2272–2281.
[27] A.C. Ferrari, D.M. Basko, Raman spectroscopy as a versatile tool for studying the properties of graphene, Nat. Nanotechnol. 8 (2013) 235–246.

[28] L.M. Malard, M.A. Pimenta, G. Dresselhaus, M.S. Dresselhaus, Raman spectroscopy in graphene, Phys. Rep. 473 (2009) 51–87.
[29] M. Rodahl, F. Höök, B. Kasemo, QCM operation in liquids: an explanation of measured variations in frequency and Q factor with liquid conductivity, Anal. Chem. 68 (1996) 2219–2227.
[30] J. Kim, S. Kwon, D.-H. Cho, B. Kang, H. Kwon, Y. Kim, S.O. Park, G.Y. Jung, E. Shin, W.-G. Kim, H. Lee, G.H. Ryu, M. Choi, T.H. Kim, J. Oh, S. Park, S.K. Kwak, S.W. Yoon, D. Byun, Z. Lee, C. Lee, Direct exfoliation and dispersion of two-dimensional materials in pure water via temperature control, Nat. Commun. 6 (2015) 8294.
[31] R. Devanathan, D. Chase-Woods, Y. Shin, D.W. Gotthold, Molecular dynamics simulations reveal that water diffusion between graphene oxide layers is slow, Sci. Rep. 6 (2016) 29484.
[32] S. Kellici, J. Acord, J. Ball, H.S. Reehal, D. Morgan, B. Saha, A single rapid route for the synthesis of reduced graphene oxide with antibacterial activities, RSC Adv. 4 (2014) 14858–14861.
[33] P. Innocenzi, L. Malfatti, D. Carboni, M. Takahashi, Sol-to-Gel transition in fast evaporating systems observed by in situ time-resolved infrared spectroscopy, ChemPhysChem 16 (2015) 1933–1939.